DNA charge neutralization by linear polymers: Irreversible binding

E. Maltsev,* J. A. D. Wattis,† and H. M. Byrne‡
Centre for Mathematical Medicine, Division of Applied Mathematics, School of Mathematical Sciences, University of Nottingham, Nottingham, NG7 2RD, UK
(Received 15 December 2005; published 6 July 2006)

We develop a deterministic mathematical model to describe the way in which polymers bind to DNA by considering the dynamics of the gap distribution that forms when polymers bind to a DNA plasmid. In so doing, we generalize existing theory to account for overlaps and binding cooperativity whereby the polymer binding rate depends on the size of the overlap. The proposed mean-field models are then solved using a combination of numerical and asymptotic methods. We find that overlaps lead to higher coverage and hence higher charge neutralizations, results which are more in line with recent experimental observations. Our work has applications to gene therapy where polymers are used to neutralize the negative charges of the DNA phosphate backbone, allowing condensation prior to delivery into the nucleus of an abnormal cell.

DOI: 10.1103/PhysRevE.74.011904 PACS number(s): 87.15.−v, 82.39.−k, 82.20.−w, 82.30.−b

I. INTRODUCTION

A. Importance of DNA charge neutralization in gene therapy

One approach to gene therapy that is being used to treat a range of inherited and acquired diseases involves the introduction of DNA into the nucleus of abnormal cells to restore their function to normal [1–4]. Delivery into such cells requires the DNA to be compacted either by polymers [5,6] or transferred within another organism, such as a virus [7,8]. Liposomes, cationic lipids [9,10], or cationic polymers such as dendrimers [5,11], polyethylenimines [12], or polyamidoamines [13,14] are all examples of nonviral vectors.

Repulsive forces from negatively charged phosphate groups which prevent DNA from forming compact structures have to be neutralized by the vector to achieve condensation. The work presented in this paper focuses on modeling charge neutralization of DNA in such nonviral gene delivery systems. It involves generalizing and solving models of random sequential absorption [15,16] using deterministic mean-field approaches, deriving expressions for the distribution of gap sizes and the overall charge neutralization.

B. Experimental observations and the counterion condensation theory

The main body of experimental work involves identifying polymers and ions that cause DNA condensation. While all studies agree that the charge of the polymers must exceed one in order for condensation to occur, they are often focused on different types of polymers. Most studies consider salt solutions and polymers of relatively small valency but there is some experimental work involving polymers with much higher charges [5,17,18]. Experiments usually focus on the charge neutralization required to condense the DNA and the morphology of the condensate.

Different polymers have been found to produce different shapes of condensate; there may be rods, toroids, and spheres. The ability to control the shape, size, and charge of the DNA-polymer complexes is important in gene therapy since these factors influence the complexes' suitability for transfection. Condensation studies performed by Roberts and co-workers [19,20] using atomic force microscopy (AFM) allow visualization of DNA movement and conformational changes. Both toroidal and extended linear structures are observed when the DNA-polymer complex condenses. In [20], the authors conclude that rings are formed from the bending of the linear structures; that the two structures exist in a dynamic equilibrium, the balance of which can be influenced by the type of polymer used.

Linear polyamines, spermidine, and spermine have been reported to employ a common molecular mechanism of DNA binding [21]. Phosphates were found to be the primary binding sites of these polyamines. It was suggested that electrostatic shielding of the phosphates causes closer helix-helix surface contacts, facilitating the condensation of DNA. DNA may also be condensed by polyamidoamine dendrimers [5]. When present in solution in excess, the dendrimers produced complexes with sufficiently large net positive charge to ensure efficient cellular uptake. In [5] the authors conclude that the most transfection-efficient complexes are not those that are the most compact but those that have highest positive charge.

Overall, the experimental evidence suggests that DNA condenses when approximately 90% of its phosphate charges are neutralized [22].

Mathematical modeling of DNA condensation has resulted in two theories that admit a description of experimental results with varying levels of accuracy and parameter fitting. The term "counterion condensation" refers to mobile positive ions being attached to negative ions that are permanently fixed to DNA [23]. Solving the Poisson-Boltzmann equation confirms the results of counterion condensation theory (see [24], for example). The equations for binding isotherms derived from approximate analytical solution of the Poisson-Boltzmann equation are given in [24]. Counterion condensation theory can be used to calculate the amount of negative DNA charge neutralized at equilibrium when

*Electronic address: Eugene.Maltsev@maths.nottingham.ac.uk
†Corresponding author; Electronic address: Jonathan.Wattis@nottingham.ac.uk
‡Electronic address: Helen.Byrne@nottingham.ac.uk

nonspecific binding of small polymers to DNA backbone occurs [22].

The second theory is the excluded-site binding model, which can be used to estimate the time variation of the charge as well as the equilibrium state and is suitable for larger polymers [13,18]. It is the second theory that is generalized in this paper.

C. Random sequential absorption and the excluded site binding model

The original model describing the binding of relatively long polymers to a number of contiguous sites of DNA was developed by McGhee and von Hippel [25]. Later, Epstein extended this work on the excluded-site binding model: in [26] an exact solution is derived for irreversible ligand binding to lattices of finite length and for studying the amount of ligand bound to a DNA molecule as a function of time; in [27] the results of Monte Carlo simulations of reversible binding are reported; and in [28] a recurrence relation for the binding capacity is derived, however, this cannot be solved explicitly. More recently, Munro *et al.* [29] tabulated data on the capacities for various lengths of polymer and DNA in the case of irreversible binding.

Alongside this mathematical modeling of the biochemical process of polymer adsorption, a similar problem has been studied by sections of the theoretical physics community. The continuous formulation of the problem of *random sequential absorption* (RSA) is equivalent to polymers of unit length landing on a molecule of infinite length and is known as the *parking problem*; it is studied in [16]. Its discrete analogue is derived by Bonnier *et al.* [15], who calculate the proportion of the infinite linear lattice covered by the landing of polymers which cover a discrete number of sites. This quantity is equivalent in our example system to the neutralization of DNA charge, which we will denote by θ.

It is argued in [30] that the excluded-site binding model of [25] has a number of deficiencies. One is that the number of sites occupied by polymer and the binding rate do not vary with salt concentration. However, in principle such effects could be included by allowing the binding rate to depend on *p*H and the concentration of the ionic species. Bossmann and Schulman [31] discuss the difficulties of interpreting experimental data on the distribution of gap sizes arising in DNA adsorption studies, and point out the different effects which may dominate in studies on small versus long strands of DNA.

Extensions of standard RSA models include cooperative sequential adsorption (CSA) where polymers preferentially attach adjacent to existing adsorbed polymers, as described by Evans [32]. While CSA leads to the higher charge neutralizations required for DNA condensation, it is hard to see the mechanism leading to cooperativity and associated preferential attachment. There are connections between models of island nucleation and growth and CSA, as noted by Evans [32] and Barma [33]. Barma [33] analyzes the dynamics of deposition and evaporation in terms of spin-chain models; these effectively allow diffusion of adsorbed particles along the substrate. Bartelt and Privman [34] and Nielaba [35] consider multilayer adsorption initially of unit length polymers, later generalizing further to consider longer polymers, mixtures, and surface diffusion following adsorption; connections with models of surface roughening and KPZ theory are noted. Such generalizations will be analyzed using our methods in forthcoming papers [36,37]. The topic of large-time asymptotics of RSA is studied by Ben-Naim and Krapivsky [38] who find exact solutions for some special cases. Krapivsky and Ben-Naim [39] consider reversible adsorption, a problem which we will analyze in a future work [36].

A variation of the model that approximates large ligands attached to polynucleotide as a one-dimensional fluid of hard rods [40] is used in [41]. However, this extension to counterion condensation theory still fails to accurately model the experimental data. It is suggested that the charge spacing decreases as more polymers are bound to polynucleotides. Only if binding rates different from the calculated ones are used can the experimental data be made to fit the theoretical binding isotherms.

DNA condensation into multi-molecular rod- or toroid-like complexes is consistent with the idea that there are attractive forces between parts of a DNA molecule (or DNA molecules) which dominate when their charge is neutralized. In some systems, the fraction of neutralized charge on the DNA has exceeded one, the DNA having attracted so much positively charged polymer that the DNA-polymer complex acquires a net positive charge. This situation is known as charge inversion. The physics of charge inversion in chemical and biological systems is reviewed in [42].

The attractive forces between circular polyions of the same charge are studied in [43,44]. Overcharging occurs because of the highly favorable gain in electrostatic free energy due to strong positional correlations between condensed counterions. The result is the appearance of purely electrostatic attraction between the like-charged macromolecules.

DNA condensation has been shown to occur when a large proportion of its negative charge is neutralized by positively charged polymers [13,20,6,22]. Since many sites become unavailable for binding, describing the interactions of a condensing polymer with the DNA from knowledge of the rate of binding of the polymer to unoccupied DNA is complicated. In particular, the overall rate of polymer binding to DNA is much larger at the start of the process, when the DNA is empty, than at later stages, when the DNA is almost fully occupied. Our irreversible binding model, based on [45], describes these features. We are not claiming to describe fully all the processes occurring as polymers adsorb to DNA, there are many effects which we ignore: for example the curvature of the DNA due to its helical form, the relative spacing of charges on the polymer may not be the same as that on the DNA, that polymers may bind at each end but not in the middle. However, our model is an extension to existing RSA-based models in that we allow partial adherence of polymers, so that overlapped binding is permitted. One of the aims of this paper is to investigate if the effects of this extra model generality are sufficient to explain the higher charge neutralizations and charge inversion that are observed in experiments and not realizable in the standard (non-overlapped-binding) RSA model.

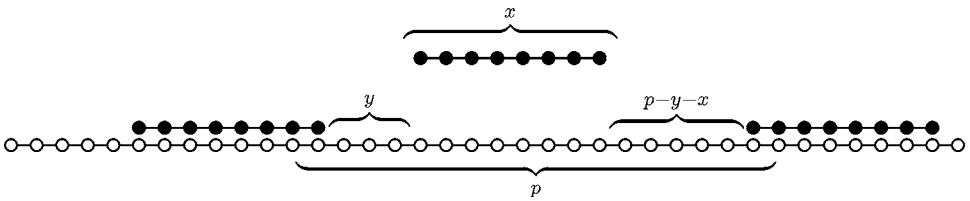

FIG. 1. Illustration of a polymer of length x attempting to land in a gap of length p on a DNA plasmid which has some sites already occupied.

D. Gap distribution model

In this work, we model the DNA as a one-dimensional strand, with uniformly spaced binding sites. The model is used to analyze how the distribution of gap sizes evolves when polymers attach to the DNA. The distribution of gap sizes allows us to calculate the fraction of DNA sites that are occupied by charged polymers and the resulting charge neutralization. We derive the governing equations by considering the general evolution of $N_p(t)$ the number of gaps of length p at time t. This may be stated as follows:

$$\frac{dN_p}{dt} = -\left(\begin{array}{c}\text{rate at which gaps of}\\ \text{length } p \text{ disappear due}\\ \text{to polymer binding}\end{array}\right) + \left(\begin{array}{c}\text{rate at which gaps of}\\ \text{length } p \text{ are created due}\\ \text{to polymer binding}\end{array}\right). \quad (1)$$

The initial irreversible binding model is derived and solved using numerical and asymptotic techniques in Sec. II. The model is then extended to allow for partially overlapped polymers (Sec. III), including the case when the binding rate depends on the gap size (Sec. IV). Following [28] recursive relations are constructed for the steady-state gap distributions that are realized in the large-time limit (Sec. II D). Using these the equilibrium charge neutralization and final distribution of gap lengths can also be calculated. The paper ends in Sec. V, with a discussion of our results and possible directions for future research.

II. BINDING WITHOUT OVERLAPS

A. Kinetics

We denote by x the length of the polymer and by p the length of the gap in which the incoming polymer will bind. Both x and p are positive integers (the unit being one base-pair). When such a polymer lands in such a gap on the DNA two smaller gaps are produced, one of length y, the second of length $p-x-y$, where $0 \leqslant y \leqslant p-x$. Thus the possibilities are as follows:

$$(p) \to (y) + (p-x-y), \quad 0 \leqslant y \leqslant p-x, \quad (2)$$

where the terms in brackets represent gaps of the corresponding size, as illustrated in Fig. 1. There are $p-x+1$ ways in which a polymer of length x can position itself in a gap of length p, provided that $p \geqslant x$. We assume that each case occurs with equal probability.

We denote the total number of gaps between polymers on the DNA by M_0 so that

$$M_0(t) = \sum_{p=0}^{P_0} N_p(t). \quad (3)$$

The number of polymers bound to the DNA is M_0-1, and the concentration of bound polymers is $B(t)=A_0[M_0(t)-1]$, where A_0 is the molar concentration of the DNA. Hence the molar concentration of free polymers $L(t)$ can be expressed as

$$L(t) = L_0 - B(t) = L_0 - A_0[M_0(t) - 1], \quad (4)$$

where $L_0=L(t=0)$ is the molar concentration of polymers in the solution before any binding occurs.

Using (2) in (1) we have the differential equations

$$\frac{dN_p}{dt} = -K_f(p-x+1)N_p \quad (P_0 - x + 1 \leqslant p \leqslant P_0), \quad (5a)$$

$$\frac{dN_p}{dt} = -K_f(p-x+1)N_p + \sum_{g=p+x}^{P_0} 2K_f N_g \quad (x \leqslant p \leqslant P_0 - x), \quad (5b)$$

$$\frac{dN_p}{dt} = \sum_{g=p+x}^{P_0} 2K_f N_g \quad (0 \leqslant p \leqslant x-1), \quad (5c)$$

where P_0 is the length of the DNA plasmid, and $K_f=k_f L(t)$ denotes the rate at which the polymer lands, k_f being a rate constant.

The sink term on the rhs of Eqs. (5a) and (5b) describes the loss of gaps of length p which are filled by incoming polymer. The source term that appears in Eqs. (5b) and (5c) describes the formation of gaps of length p when polymer lands in a gap of length $g>p$. The factor of 2 is due to the fact that two gaps are formed when a landing event occurs. Since gaps of length p for which $P_0-x+1 \leqslant p \leqslant P_0$ can only be destroyed, Eqs. (5a) contains just a sink term. By contrast, since gaps of length $p<x$ are too small to admit a polymer, no sink term is included in Eq. (5c).

At $t=0$, we assume that no polymer has been bound and so simulations are performed with the initial condition $N_p(0)=\delta_{p,P_0}$ (using the Kronecker δ notation).

B. Charge neutralization

As polymers adhere, they neutralize the negative charge of the DNA. Two physical quantities derived from the gap size distribution can be used to calculate the extent of charge neutralization. They are the total number of gaps, M_0, as defined by (3) and the total length of gaps, M_1, defined by

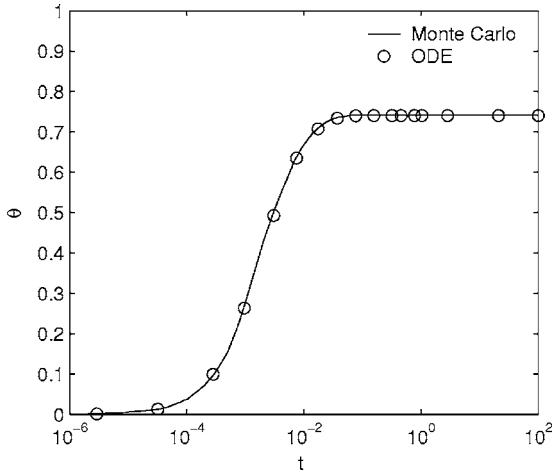

FIG. 2. Evolution of charge neutralization θ calculated from Eq. (5) and compared to Monte Carlo simulation results. Parameter values: $L_0=8$, $A=1$, $P_0=20$ sites, $x=5$ sites, and $k_f=10\ \mathrm{s}^{-1}$.

$$M_1(t)=\sum_{p=1}^{P_0} pN_p(t). \tag{6}$$

The charge neutralization θ is defined to be the proportion of charges on the DNA neutralized by the polymer. This can be calculated in two ways:

$$\theta(t)=\frac{x(M_0(t)-1)}{P_0}=\frac{P_0-M_1(t)}{P_0}, \tag{7}$$

since M_0-1 is the number of polymer molecules attached to the DNA plasmid and P_0-M_1 is the total number of sites occupied by the polymers. We thus have the identity

$$xM_0(t)+M_1(t)=P_0+x, \tag{8}$$

which is valid for all t.

C. Numerical solution

Equations (5) were solved using a semi-implicit extrapolation method [46] with adaptive step-size control written and compiled using Fortran 90. The charge neutralization θ was then calculated using Eq. (7).

The evolution of the charge neutralization for a typical simulation is plotted in Fig. 2. The accuracy of the numerical solution is confirmed by comparing it to results from a Monte Carlo simulation with the same parameters [47]. From Fig. 2 we note in both cases a rapid approach to an equilibrium charge neutralization.

D. Irreversible equilibrium asymptotics

A recursive relation, developed in [28], allows us to calculate the equilibrium binding capacity, $R(x,P_0)$. This is the average number of polymers of length x that irreversibly bind to DNA of length P_0. $R(x,P_0)$ corresponds to an equilibrium value of $M_0(t)-1$ from Sec. II [Eq. (3)]. Clearly if the DNA is shorter than the polymer ($P_0<x$), then no polymers can land and so $R(x,P_0)=0$. If $x\leqslant P_0<2x$, then only one polymer can be accommodated so that $R(x,P_0)=1$. For longer DNA chains ($P_0\geqslant 2x$) the number of polymers landing will depend upon precisely where earlier polymers landed. When a polymer lands on a lattice of length P_0, two shorter sublattices are generated. The total capacity of the long lattice is one more than the sum of the capacities of the two shorter lattices. By conditioning on the landing site, the recursive relation

$$R(x,P_0)=1+\frac{2\sum_{q=x}^{P_0-x}R(x,q)}{P_0-x+1}\quad (2x\leqslant P_0), \tag{9a}$$

$$R(x,P_0)=1\quad (x\leqslant P_0<2x), \tag{9b}$$

$$R(x,P_0)=0\quad (P_0<x), \tag{9c}$$

for the expected capacity can be derived. In Eqs. (9) we view P_0 as the recurrence parameter. We now derive a recurrence relation for $R(x,P_0)$. From (9a) we have that

$$R(x,P_0-1)=1+2\frac{-R(x,P_0-x)+\sum_{p=x}^{P_0-x}R(x,p)}{P_0-x}, \tag{10}$$

which, upon rearranging, yields

$$2\sum_{p=x}^{P_0-x}R(x,p)=(P_0-x)[R(x,P_0-1)-1]+2R(x,P_0-x). \tag{11}$$

By substituting from (11) into (9) and noting that $R(x,P_0)$ can be calculated explicitly for $P_0\leqslant 3x-1$, we deduce

$$R(x,P_0)=1+\frac{(P_0-x)(R(x,P_0-1)-1)+2R(x,P_0-x)}{P_0-x+1}\quad (3x\leqslant P_0), \tag{12a}$$

$$R(x,P_0)=1+2\left(\frac{P_0-2x+1}{P_0-x+1}\right)\quad (2x\leqslant P_0<3x), \tag{12b}$$

$$R(x,P_0)=1\quad (x\leqslant P_0<2x), \tag{12c}$$

$$R(x,P_0)=0\quad (P_0<x). \tag{12d}$$

Equation (12a) is an xth-order recurrence relation in P_0, with P_0-dependent coefficients, for which an explicit solution is not available.

We are interested in the behavior of solutions when the polymers occupy many base pairs and the DNA is many times longer than the polymer, that is, $1\ll x\ll P_0$. There are many such scalings, and so for the purposes of giving illustrative calculations we choose one particular limit, namely that of $P_0=\mathrm{O}(x^2)\gg 1$. Accordingly we define a small parameter, ϵ, by $\epsilon=1/x\ll 1$. We assume that $P_0\sim O(\epsilon^{-2})$ and write $y=\epsilon^2 P_0$, where $y\sim O(1)$. This scaling is typical of those used

in experiments on DNA condensation by cationic polymers where the DNA plasmid is typically of length 10^4 base pairs and polymers are of length 10^2 units.

If $\theta \sim O(1)$, then, using Eq. (7), $R=P_0\theta/x \sim O(1/\epsilon)$, that is, a plasmid of length $O(1/\epsilon^2)$ can accept $O(1/\epsilon)$ polymers of length $O(1/\epsilon)$. We therefore rescale the irreversible binding capacity as $R(x,P_0)=r(y)/\epsilon$ with $r \sim O(1)$. We substitute x, P_0, and R in Eq. (12a) to yield

$$\left(\frac{y}{\epsilon^2}-\frac{1}{\epsilon}+1\right)r(y)=\epsilon+\left(\frac{y}{\epsilon^2}-\frac{1}{\epsilon}\right)r(y-\epsilon^2)+2r(y-\epsilon). \tag{13}$$

We construct an asymptotic expansion for $r(y)$ approximating $r(y-\epsilon)$ by $r(y)-\epsilon\frac{d}{dy}r(y)$ since $y \sim O(1)$. Making this approximation and retaining only terms of leading order and first order yields the following ordinary differential equation (ODE) for $r(y)$:

$$(y+\epsilon)\frac{dr(y)}{dy}=r(y)+\epsilon, \tag{14}$$

with solution

$$r(y)=c(y+\epsilon)-\epsilon, \tag{15}$$

for some constant c. Rewriting (15) in terms of the original variables yields

$$\theta(x,P_0)=\theta(x,\infty)-\frac{x}{P_0}[1-\theta(x,\infty)], \tag{16}$$

where the constant $\theta(x,\infty)$ is determined by matching Eq. (16) to the largest solution of Eq. (12) that is easily obtained analytically.

From Eq. (12b), the largest value of P_0 for which we can determine $R(x,P_0)$ without using the recurrence relation occurs when $P_0=3x-1$. Substituting $R(x,3x-1)=2$ in Eq. (16) gives

$$\theta(x,3x-1)=\theta(x,\infty)-\frac{x}{3x-1}[1-\theta(x,\infty)]=\frac{2x}{3x-1}, \tag{17}$$

which, on rearrangement, yields

$$\theta(x,\infty)=\frac{3x}{4x-1}. \tag{18}$$

Substitution of $\theta(x,\infty)$ in Eq. (16) yields the following expression for the charge neutralisation of DNA molecules having at least $3x$ sites

$$\theta(x,P_0)=\frac{3x}{4x-1}\left(1-\frac{x-1}{3P_0}\right). \tag{19}$$

In Fig. 3 the asymptotic solution (19) is shown to be in very close agreement with the exact recurrence relations over a range of values for DNA length P_0.

Equation (19) implies that when polymers bind irreversibly without overlaps the highest charge neutralization occurs when $x=2$ and $\theta(2,\infty)=0.86$. Such neutralization is insufficient to condense DNA. Applying Eq. (19) to the continuous parking problem results in $\lim_{x\to\infty,P_0\to\infty}\theta(x,P_0)=0.750$, which is close to the solution obtained in [16], where $\theta=0.748$.

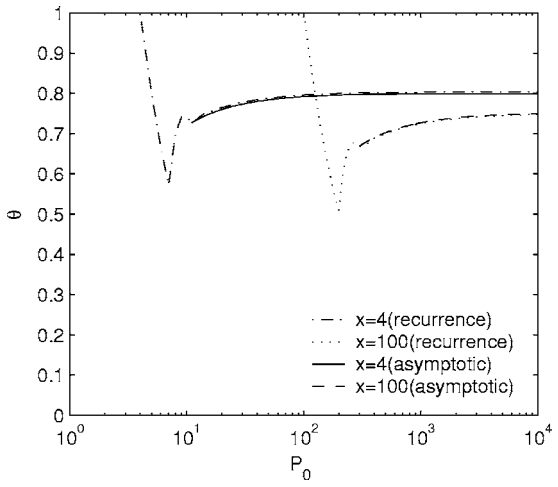

FIG. 3. Exact charge neutralization θ when nonoverlapped polymers that occupy 4 and 100 sites bind irreversibly to DNA of various lengths P_0. There is excellent agreement between the asymptotic results and those obtained from the recurrence relation.

From [48], the kinetics of the neutralization of charge for a lattice of infinite length are

$$\theta(x,t)=\int_0^{x[1-\exp(-k_f t)]}\exp\left(-2\int_0^u\frac{1-(1-v/x)^{x-1}}{v}dv\right)du, \tag{20}$$

where k_f is the binding rate.

In Fig. 4 the asymptotic solution (19) is plotted and shown to be in good agreement with exact solutions compiled in [48] of the equilibrium charge neutralization that were obtained by evaluating Eq. (20) in the limit $t=\infty$.

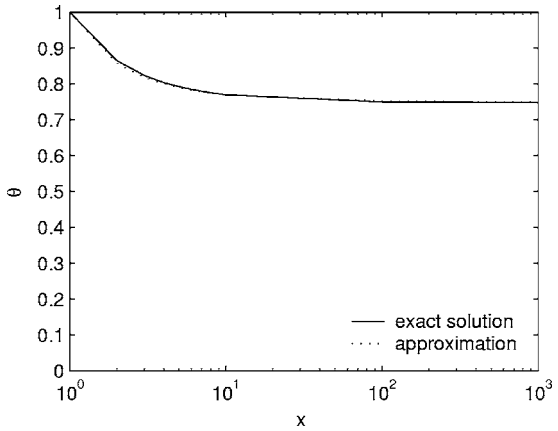

FIG. 4. Diagram showing how the charge neutralization changes as the length of the polymer varies when the polymer binds irreversibly and with no overlaps to a strip of DNA of infinite length.

E. Equilibrium gap length distribution

By generalizing the argument presented in the previous section it is possible to derive recurrence relations for the equilibrium distribution of gaps, that is $\lim_{t\to\infty} N_p(t)$, which we shall now denote by $N_p^{\mathrm{eq}}(x,P_0)$, explicitly stating the dependence of N_p^{eq} on x and P_0. Irreversible binding without overlaps results in all gaps larger than $x-1$ being filled by polymers so that $N_p^{\mathrm{eq}}(x,P_0)=0$ for $p\geqslant x$. As stated in Sec. II D, an empty DNA molecule of length P_0 has P_0-x+1 landing positions for a polymer of length x. Each point of initial attachment results in two sublattices, a sublattice and a gap, or two gaps. Here, by "gap" we mean a gap of size $p<x$ and by "sublattice" we mean a gap of size $p\geqslant x$ which will be further subdivided by the binding of more polymers.

The total number of gaps is calculated recursively by considering the distribution of gap sizes on smaller sublattices:

$$\begin{pmatrix}\text{Number of gaps}\\ \text{of length } p \text{ on}\\ \text{plasmid of length } P_0\end{pmatrix} = 2\frac{\begin{pmatrix}\text{Possibility of gap}\\ \text{generation on}\\ \text{the first landing}\end{pmatrix} + \begin{pmatrix}\text{Sum of all gaps of size } p\\ \text{from sub-lattices of DNA}\\ \text{formed by the landing}\end{pmatrix}}{\begin{pmatrix}\text{Total number of}\\ \text{landing positions}\end{pmatrix}}. \tag{21}$$

The resulting recursive relation for the distribution of gaps of length $(0\leqslant p\leqslant x-1)$ is

$$N_p^{\mathrm{eq}}(x,P_0)=\frac{2}{(P_0-x+1)}\left(1+\sum_{q=x+p}^{P_0-x}N_p^{\mathrm{eq}}(x,q)\right), \quad (p+2x\leqslant P_0), \tag{22a}$$

$$N_p^{\mathrm{eq}}(x,P_0)=\frac{2}{P_0-x+1} \quad (p+x\leqslant P_0<p+2x), \tag{22b}$$

$$N_p^{\mathrm{eq}}(x,P_0)=0 \quad (P_0<p+x). \tag{22c}$$

Using an argument similar to that used to derive Eq. (12), Eq. (22) can be rewritten as an xth-order recurrence relation:

$$N_p^{\mathrm{eq}}(x,P_0)=\frac{(P_0-x)N_p^{\mathrm{eq}}(x,P_0-1)+2N_p^{\mathrm{eq}}(x,P_0-x)}{P_0-x+1} \quad (p+x<P_0), \tag{23a}$$

$$N_p^{\mathrm{eq}}(x,P_0)=\frac{2}{P_0-x+1} \quad (P_0=p+x), \tag{23b}$$

$$N_p^{\mathrm{eq}}(x,P_0)=0 \quad (P_0<p+x). \tag{23c}$$

A typical case is presented in Fig. 5, where the equilibrium gap distribution $N_p^{\mathrm{eq}}(x,P_0)$ is plotted for fixed values of x and P_0. The log-scale plot in Fig. 5(b) suggests that the distribution is approximately of the form $N_p=a-b\log p$ (where a and b are constants).

III. OVERLAPPED BINDING

Experimental results suggest that at equilibrium a net resultant positive charge can arise when positively charged polymers land on negatively charged DNA [49]. One explanation of this phenomenon is that some polymers are only partially bound to the DNA surface. This could occur when polymers attach to gaps on the DNA which are shorter in length than the polymers (see Fig. 6).

In this section we consider polymer-binding with overlaps, assuming as before that the binding rate is independent of the length of the binding region.

A. Kinetics

As before, when a polymer of length x lands in a gap of width p, two smaller gaps are produced, one of length y and the other of length $p-x-y$. The possibilities are as follows

$$(p)\to(y)+(p-x-y), \quad 1-x\leqslant y\leqslant p-1. \tag{24}$$

Negative values of y and $p-x-y$ correspond to regions where there is an overlap of length $-y$ or $-(p-x-y)$. Polymers cannot land in "negative" gaps: they are only formed when polymers land.

As illustrated in Fig. 6, a polymer can bind in a gap of length $p>0$ in $p+x-1$ ways. If the polymers land on the DNA plasmid at the rate K_f, then gaps of size p are removed at a rate $-K_f(p+x-1)N_p$, which is proportional to the number of possible landing positions and the number of such gaps, N_p. As in Sec. II, the assumption that the polymer lands on the DNA plasmid at the rate K_f means that the rate at which gaps of size p are created is given by $2K_f\Sigma_{g=p+1}^{P_0}N_g$. The resulting equations are

$$\frac{dN_p}{dt}=-K_f(p+x-1)N_p \quad (p=P_0), \tag{25a}$$

$$\frac{dN_p}{dt}=-K_f(p+x-1)N_p+\sum_{g=p+1}^{P_0}2K_fN_g \quad (1\leqslant p\leqslant P_0-1), \tag{25b}$$

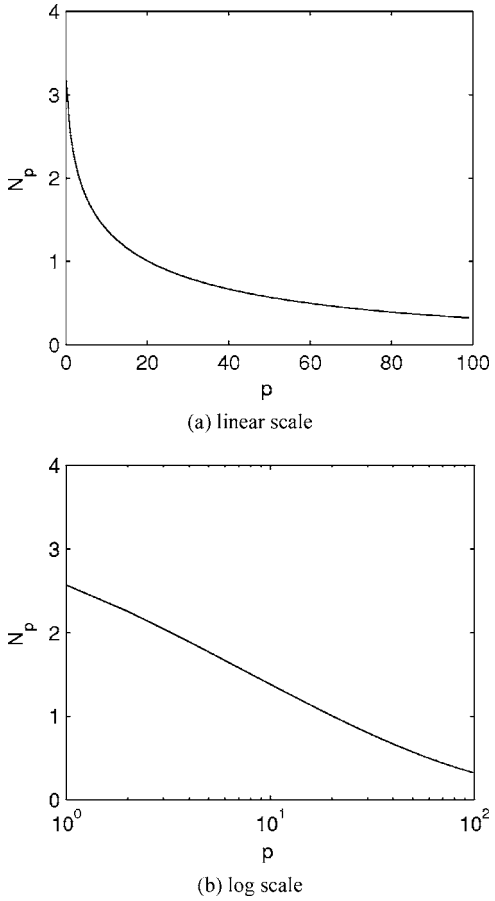

FIG. 5. Series of plots showing the equilibrium gap distribution when binding is irreversible, with no overlaps. Parameter values: $P_0=10\,000$ and $x=100$ ($\theta=0.7473$).

$$\frac{dN_p}{dt} = \sum_{g=1}^{P_0} 2K_f N_g \quad (1-x \leqslant p \leqslant 0). \tag{25c}$$

Although Eqs. (25) appear to be identical to (5), their domains of applicability in p space differ, and the factors of $p-x+1$ have been replaced by $p+x-1$. In both cases gaps of length P_0 cannot be created as binding leads only to the formation of smaller gaps. Gaps of size $1 \leqslant p \leqslant P_0-1$ may be created and destroyed. Once a gap of zero, or negative size, is created, no further binding event can remove it; therefore such gaps can only be created. Since we allow overlaps to occur, the lower limit of the sum appearing in Eqs. (25) is $g=1$ rather than $g=p+1$. This is because the smallest gap into which a polymer may land has size 1.

As in the case of nonoverlapped binding (8), we have $M_1(t)+xM_0(t)=P_0+x$, and

$$\theta = \frac{x(M_0-1)}{P_0} = 1 - \frac{M_1}{P_0}. \tag{26}$$

However, M_0 and M_1 are now defined slightly differently: in place of (3) and (6) we have

$$M_0(t) = \sum_{p=1-x}^{P_0} N_p(t), \quad M_1(t) = \sum_{p=1-x}^{P_0} pN_p(t), \tag{27}$$

thus $M_0(t) \geqslant 0$, but $M_1(t) < 0$ is allowable, leading to the possibility that $\theta > 1$ in (26).

B. Numerical solution

As in Sec. II C, Eqs. (25) were solved using a semi-implicit extrapolation method with adaptive step-size control. The charge neutralization corresponding to a numerical solution of Eqs. (25) is plotted in Fig. 7 for the binding of a five-site polymer to a strip of DNA of length 200. We observe much greater charge neutralization when overlapping occurs.

The equilibrium gap distributions corresponding to the simulations presented in Fig. 7 are plotted in Fig. 8 and show that overlapped irreversible binding results in a uniform distribution of overlaps. This surprising result is due to the unrealistic assumption that the adherence rate of polymers does not depend on the number of bonds that form (that is, the size of the gap in which the polymer lands). A more realistic scenario in which the rate of adherence depends on gap size is analyzed in the next section.

C. Equilibrium plasmid capacity

It is possible to construct a recursive relation for the equilibrium binding capacity of a strip of DNA when polymers bind irreversibly with overlaps (i.e., the equilibrium solution of the model presented in Sec. III A). The derivation is similar to that presented in Sec. II D, except that binding can now

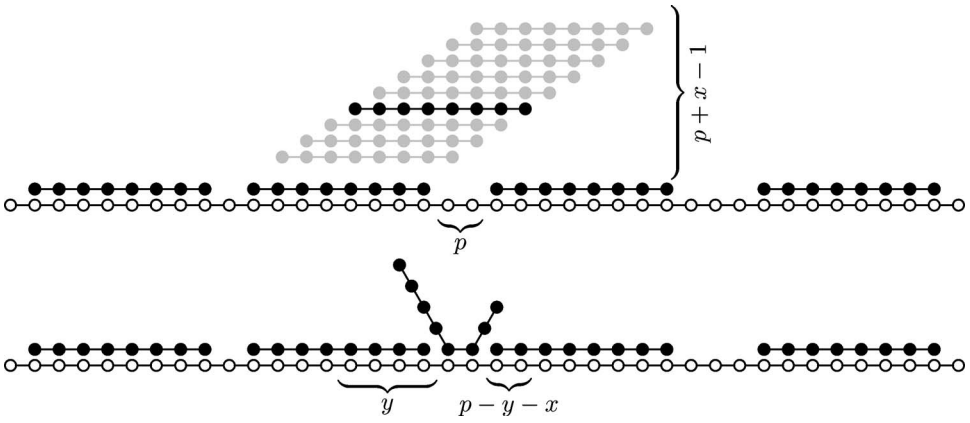

FIG. 6. There are $p+x-1$ possible landing positions (shown in upper panel, in gray) for a polymer of length x binding to DNA in a gap of width $p<x$.

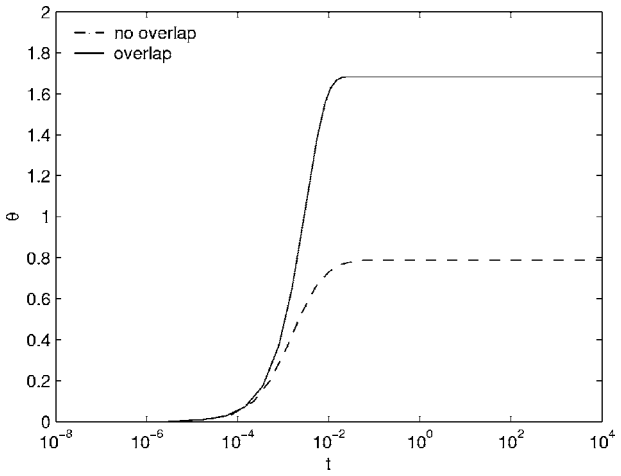

FIG. 7. Plot showing how for irreversible binding the charge neutralization changes when binding with overlaps occurs. Parameter values: $L_0=10^{-6}$ M, $A=5\times10^{-9}$ M, $P_0=200$ sites, $x=5$ sites, $k_f=10^8$ M^{-1} s^{-1}.

occur in any gap on the DNA of length greater than zero. It follows that there are P_0+x-1 landing positions for polymer of length x landing on a stretch of DNA of length P_0. Therefore the average number of polymers of length x that bind irreversibly (with overlaps) to a DNA of length P_0 is

$$R(x,P_0) = 1 + \frac{2\sum_{p=1}^{P_0-1} R(x,p)}{P_0+x-1}. \tag{28}$$

We remark that the minimum gap length that can accommodate another polymer has decreased from x in Eq. (9) (lower limit of the sum) to 1. The largest gap created by the landing polymers has also increased from P_0-x to P_0-1 (upper limit of the sum). Since DNA of length $P_0=1$ always accepts just one polymer, we impose the boundary condition

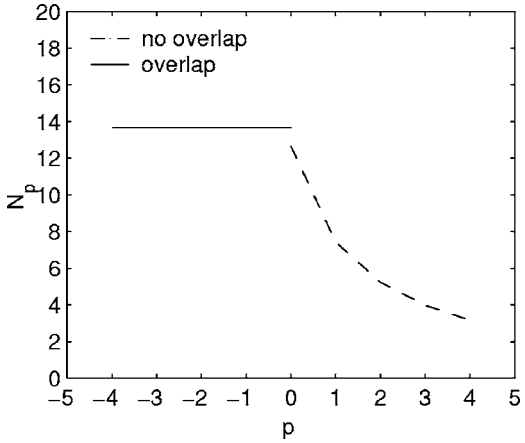

FIG. 8. Plot showing how for irreversible binding the equilibrium gap distribution changes when binding with overlaps occurs. Parameter values: as per Fig. 7.

$$R(x,1) = 1, \tag{29}$$

and we may use (29) to simplify Eq. (28) to obtain

$$R(x,P_0) = 1 + \frac{2(P_0-1)}{x+1}. \tag{30}$$

It follows from (30) that the fraction of neutralized charge is

$$\theta(x,P_0) = \frac{x}{P_0}\left(1+\frac{2(P_0-1)}{x+1}\right) = 1 + \frac{(x-1)(P_0+x)}{P_0(x+1)}, \tag{31}$$

so that charge inversion occurs for all $x>1$ and

$$\theta \sim 2 + \frac{x}{P_0}, \tag{32}$$

as $P_0\to\infty$ and $x\to\infty$, with x/P_0 fixed. For $x=O(1)$ and $P_0\to\infty$, we have

$$\theta \sim 2 - \frac{2}{x+1}. \tag{33}$$

It is possible to combine Eqs. (32) and (33) by considering the asymptotic limit $P_0\gg1$ with $x\sim\sqrt{P_0}$, since then Eq. (31) yields

$$\theta \sim 2 - \frac{2}{x} + \frac{x}{P_0}. \tag{34}$$

The scaling $P_0=O(x^2)\gg1$ was chosen in Sec. II D as *an* example of $P_0\gg x\gg1$ due to its applicability to polymer adsorption onto a DNA substrate. We see from (34) that the scaling $P_0\sim x^2\gg1$ is a useful example in that it simultaneously illustrates both the effects (32), which occurs for $P_0\sim x\gg1$, and (33), which holds when $P_0\gg x\sim1$.

Figure 9 shows how θ varies with x for DNA of length 10^4 sites. As expected from (31), charge inversion is evident for all values of $x>1$ and θ increases with x.

Figure 10 displays a series of curves showing how, for a given polymer of fixed length, the equilibrium charge neutralization varies when the length of the DNA is altered. We note that $\theta\to1+(x-1)/(1+x)$ as $P_0\to\infty$, with $x=O(1)$, as expected from Eq. (33).

D. Equilibrium gap length distribution

To find the equilibrium gap distribution when overlaps occur we use a similar technique to that described above for θ. A polymer of length x can land on an empty DNA plasmid of length P_0 in P_0-x+1 ways, as in the case of nonoverlapped binding. In addition, there are $x-1$ landing positions on each side of the DNA plasmid which result in an overlapping. Thus, following arguments similar to those preceding Eq. (22), we obtain the recursive relation

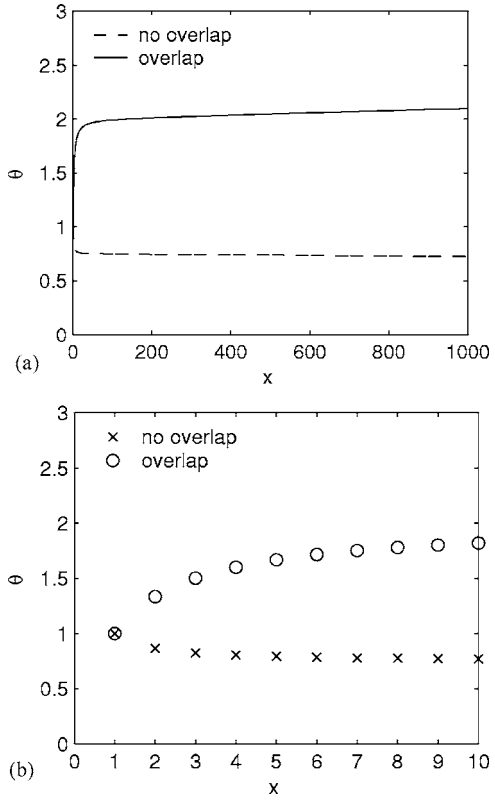

FIG. 9. Equilibrium charge neutralization θ, as defined by Eq. (31), when polymers of length x bind irreversibly to DNA of length $P_0=10^4$. In (a) the charge neutralization θ is plotted for the range of polymer lengths $1\leqslant x\leqslant 1000$, showing a region of rapid variation for smaller x. In (b) we focus on the range $1\leqslant x\leqslant 10$, showing that the two cases coincide at $x=1$.

$$N_p^{\mathrm{eq}}(x,P_0)=\frac{2}{(P_0+x-1)}\left(1+\sum_{q=1}^{P_0-1}N_p^{\mathrm{eq}}(x,q)\right)\quad(1<P_0),\tag{35}$$

for the gap distribution $(1-x\leqslant p\leqslant 0)$, with $N_p^{\mathrm{eq}}(x,1)=2/x$, since only one polymer binds to DNA of length $P_0=1$ and it can do so in x different ways, leading to gaps of size p and $1-p-x(1-x\leqslant p\leqslant 0)$, each of which are equally likely. The recurrence relation and the initial condition are independent of p. Therefore, when overlapped binding occurs at a constant rate, the equilibrium gap distribution is uniform.

Equation (35) can be simplified by noting that

$$N_p^{\mathrm{eq}}(x,P_0-1)=\frac{2}{(P_0+x-2)}\times\left(1+\sum_{q=1}^{P_0-1}N_p^{\mathrm{eq}}(x,q)-N_p^{\mathrm{eq}}(x,P_0-1)\right);\tag{36}$$

combining (35) and (36) it follows that

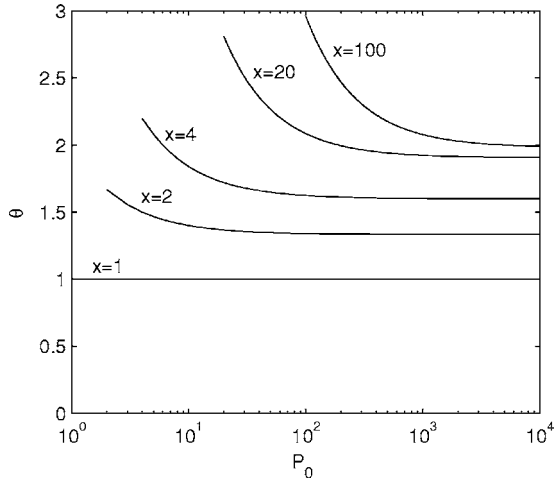

FIG. 10. Series of curves showing how, for polymers of fixed length x, the equilibrium charge neutralisation θ varies with P_0, the length of the DNA plasmid.

$$N_p^{\mathrm{eq}}(x,P_0)=\left(\frac{P_0+x}{P_0+x-1}\right)N_p^{\mathrm{eq}}(x,P_0-1)\quad(1<P_0),\tag{37a}$$

$$N_p^{\mathrm{eq}}(x,1)=\frac{2}{x}.\tag{37b}$$

Equation (37) can be solved to give

$$N_p^{\mathrm{eq}}(x,P_0)=\left(\frac{P_0+x}{1+x}\right)N_p^{\mathrm{eq}}(x,1)=\frac{2(P_0+x)}{x(x+1)},\tag{38}$$

which we note is independent of gap size p. It is also possible to calculate the charge neutralization. Suppose that the average gap length is L. Then $M_1=LM_0$ (note $L<0$, $M_0>0$, $M_1<0$). The fraction of neutralized charge is then

$$\theta=\frac{(P_0-L)}{P_0}\frac{x}{(x+L)}=\frac{1-L/P_0}{1+L/x}.\tag{39}$$

Now we recall that $xM_0+M_1=P_0+x$ [see Eq. (8)]. Since there is an equal number of gaps of every length, the average gap length L satisfies

$$L=\frac{1}{x}\sum_{i=1-x}^{0}i=\frac{1-x}{2},\tag{40}$$

as expected for a uniform distribution on $1-x\leqslant p\leqslant 0$. Substitution of L in Eq. (39) confirms Eq. (31).

IV. IRREVERSIBLE BINDING WITH OVERLAP-DEPENDENT RATES

A. Kinetics

It is reasonable to assume that a polymer is less likely to bind to the DNA if the location where it binds is partially occupied by other polymers. We account for this effect by allowing the binding rate K_f to vary with p, the number of bonds formed, in the following way:

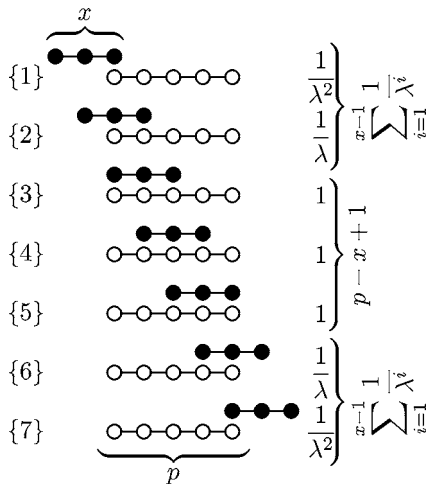

FIG. 11. Overlap-length cooperativity of overlapped landing ($x=3$, $p=5$).

$$K_f^{(p)} = \frac{K_f}{\lambda^{x-p}} \quad (p \leqslant x). \tag{41}$$

In (41) λ is the binding cooperativity constant. If the polymer is positioned so that all x bonds form, then $K_f^{(x)}=K_f$. The binding rate is reduced if the gap between polymers already attached to the DNA is not large enough to accept the full length of the landing polymer: every time the gap size is reduced by one site, it is decreased by a factor of λ. Hence the lowest nonzero adhesion rate corresponds to a polymer landing and binding to the DNA in a gap of unit length, which occurs at a rate $K_f^{(x)}/\lambda^{x-1}$. Varying λ from unity to infinity interpolates between the previously described models of overlapped binding ($\lambda=1$) and binding without overlaps ($\lambda=\infty$). Typically we expect λ to be close to unity. This is because the probability of forming each individual bond is high, but sufficiently far away from unity that the probability of forming all x bonds is distinct from unity. Treating each bond-formation event as independent, which we acknowledge is an approximation, the probability of forming p bonds is λ^p. Other choices for $K_f^{(p)}$ could be made, for example $K_f^{(p)}=K_f(p/x)^\nu$ with $\nu>0$.

1. Destruction of gaps by polymer binding

We now assume that the rate of binding depends on the number of sites at which the polymer binds. Figures 11 and 12 illustrate all the contributions to the sink terms of the binding kinetics equations. When the gap is longer than the polymer (i.e., $p>x$) there are $p+x-1$ sites at which a polymer can bind partially if we allow overlaps. This contrasts with $p-x+1$ sites at which the polymer may bind when overlaps are not allowed. The binding rate depends on the number of sites to which the polymer attaches. Individual binding rates corresponding to each position and expressions combining them are displayed on the rhs of Fig. 11. The rate at which gaps of length p are removed is obtained by summing all the possible binding rates and in this case it results in

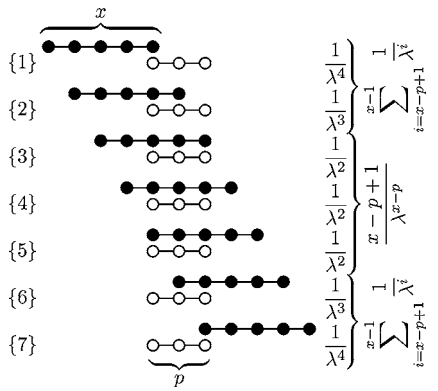

FIG. 12. Overlap-length cooperativity of overlapped landing ($x=5$, $p=3$).

$$\begin{pmatrix}\text{rate at which gaps of}\\ \text{length } p \text{ are removed}\end{pmatrix} = K_f\left(p-x+1+2\sum_{i=1}^{x-1}\frac{1}{\lambda^i}\right)N_p$$
$$= K_f\left(p-x+1+\frac{2(1-\lambda^{1-x})}{\lambda-1}\right)N_p. \tag{42}$$

When the gap is smaller than the polymer $p<x$ (Fig. 12) then any polymer that attaches will bind partially. As a result, the rate at which gaps of length $p<x$ form depends on the number of bound sites; there are still $p+x-1$ binding configurations.

When the polymer fully covers the gap, the number of overlapped sites is $x-p$ and hence the binding rate is

$$K_f^{(p)} = \frac{K_f}{\lambda^{x-p}}.$$

Since there are $x-p+1$ such positions, the contribution to the rate of destruction of gaps from polymers that fully cover the gap is

$$K_f\lambda^{p-x}(x-p+1)N_p. \tag{43}$$

Polymers that partially cover the gap contribute as follows to gap destruction:

$$2K_f\left(\sum_{i=x-p+1}^{x-1}\frac{1}{\lambda^i}\right)N_p = K_f\left(\frac{2(\lambda^{p-1}-1)}{\lambda^{x-1}(\lambda-1)}\right)N_p. \tag{44}$$

Combining (43) and (44) we deduce that the rate at which gaps of length $1\leqslant p\leqslant x$ are destroyed is given by

$$K_f\left(\frac{2\lambda^{1-x}(\lambda^{p-1}-1)}{\lambda-1}+\lambda^{p-x}(x-p+1)\right)N_p. \tag{45}$$

2. Creation of gaps and overlaps by polymer-binding

A gap of length $1-x\leqslant p\leqslant 0$ is created when a polymer binds partially to a gap of length $1\leqslant g\leqslant p+x$ (illustrated in Fig. 13) by g sites only. It follows from (41) that the binding rate is $K_f^{(x)}/\lambda^{x-g}$ and the contribution to the creation of gaps is

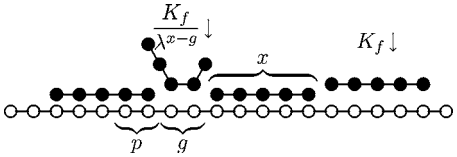

FIG. 13. An overlap of the length p created inside of the short gap of the length g.

$$2K_f \sum_{g=1}^{p+x} \frac{N_g}{\lambda^{x-g}}. \tag{46}$$

When larger gaps of length $p+x+1 \leqslant g \leqslant P_0$ are destroyed, and the only sites where the polymer does not bind are due to the overlaps, then the binding rate is $K_f^{(x)}/\lambda^{-p}$ (see Fig. 14) and the contribution to the creation of gaps is

$$2K_f \sum_{g=p+x+1}^{P_0} \frac{N_g}{\lambda^{-p}}. \tag{47}$$

If a gap of length $1 \leqslant p \leqslant P_0 - x - 1$ is created when a polymer binds to a gap of length $p+1 \leqslant g \leqslant p+x$, then the polymer is attached by $g-p$ sites only (see Fig. 15). It follows from (41) that the binding rate is $K_f^{(x)}/\lambda^{p+x-g}$ and the contribution to the creation of gaps is

$$2K_f \sum_{g=p+1}^{p+x} \frac{N_g}{\lambda^{p+x-g}}. \tag{48}$$

When larger gaps of length $p+x+1 \leqslant g \leqslant P_0$ are destroyed, leaving a gap of size p, with no overlaps being formed, the binding rate is $K_f^{(x)}$ (see Fig. 16) and the contribution to the creation of gaps is

$$2K_f \sum_{g=p+x+1}^{P_0} N_g. \tag{49}$$

Larger gaps of length $P_0 - x \leqslant p \leqslant P_0 - 1$ can only be created by partially bound polymers which attach with $g-p$ sites. It follows from (41) that the binding rate is $K_f^{(x)}/\lambda^{p+x-g}$ and the contribution to the creation of gaps is the same as (48) with the upper limit of the sum set to P_0 as the length of the DNA limits the size of the gap being destroyed:

$$2K_f \sum_{g=p+1}^{P_0} \frac{N_g}{\lambda^{p+x-g}}. \tag{50}$$

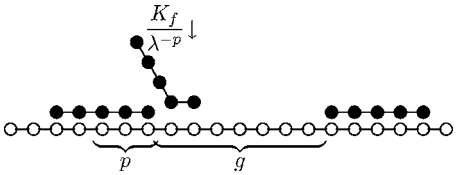

FIG. 14. An overlap of length p is created when a polymer partially binds inside a gap of length g.

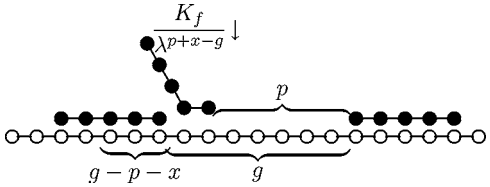

FIG. 15. A gap of length p is created when a polymer partially binds inside a gap of the length g.

Using the above results we deduce that when Eqs. (5) and (25) are adjusted to allow for overlap-dependent binding rates, the following system of differential equations is obtained:

$$\frac{dN_p}{dt} = -K_f N_p \left(p - x + 1 + \frac{2(1-\lambda^{1-x})}{\lambda - 1} \right) \quad (p = P_0), \tag{51a}$$

$$\frac{dN_p}{dt} = -K_f N_p \left(p - x + 1 + \frac{2(1-\lambda^{1-x})}{\lambda - 1} \right) + 2K_f \sum_{g=p+1}^{P_0} \frac{N_g}{\lambda^{p+x-g}} \quad (P_0 - x \leqslant p \leqslant P_0 - 1), \tag{51b}$$

$$\frac{dN_p}{dt} = -K_f N_p \left(p - x + 1 + \frac{2(1-\lambda^{1-x})}{\lambda - 1} \right) + 2K_f \sum_{g=p+x+1}^{P_0} N_g + 2K_f \sum_{g=p+1}^{p+x} \frac{N_g}{\lambda^{p+x-g}} \quad (x+1 \leqslant p \leqslant P_0 - x - 1), \tag{51c}$$

$$\frac{dN_p}{dt} = -K_f \left(\frac{2\lambda^{1-x}(\lambda^{p-1}-1)}{\lambda - 1} + \lambda^{p-x}(x-p+1) \right) N_p + 2K_f \sum_{g=p+x+1}^{P_0} N_g + 2K_f \sum_{g=p+1}^{p+x} \frac{N_g}{\lambda^{p+x-g}} \quad (1 \leqslant p \leqslant x), \tag{51d}$$

$$\frac{dN_p}{dt} = 2K_f \sum_{g=p+x+1}^{P_0} \frac{N_g}{\lambda^{-p}} + 2K_f \sum_{g=1}^{p+x} \frac{N_g}{\lambda^{x-g}} \quad (1 - x \leqslant p \leqslant 0). \tag{51e}$$

A semi-implicit extrapolation method was used to solve the system of equations (51). Figure 17 shows how the charge neutralization evolves for different values of the bind-

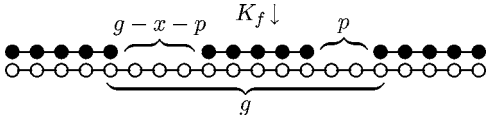

FIG. 16. A gap of length p is created when a polymer lands inside a gap of length g.

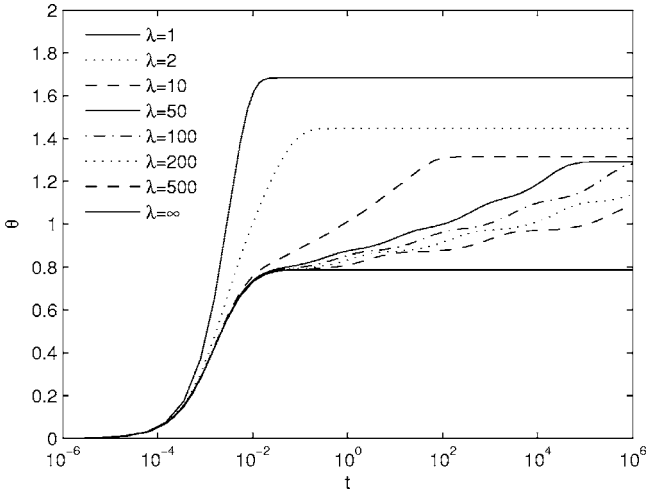

FIG. 17. Series of curves showing how the dynamics of the charge neutralization change for irreversible binding with different binding cooperativity constants λ. Binding with no overlaps (λ $=\infty$) corresponds to the lowest curve and λ$=1$ where overlapped binding is not penalized in any way corresponds to the top curve. Parameter values: $L_0=10^{-6}$ M, $A=5\times10^{-9}$ M, $x=5$ sites, $P_0=200$ sites, $k_f=10^8$ M^{-1} s^{-1}.

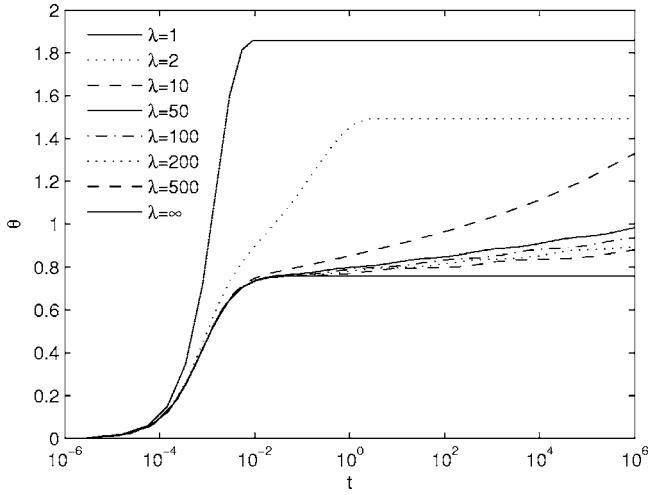

FIG. 18. Irreversible binding with different binding cooperativity constants. Parameter values: as per Fig. 17, except $x=10$ sites.

ing cooperativity constant, λ, when a polymer of length $x=5$ binds to a DNA plasmid of length $P_0=200$. The uppermost curve in Fig. 17 corresponds to overlapped binding at a rate that is independent of the size of the landing site (λ $=1$) as in Sec. III and has a shape similar to the plot of binding without overlaps ($\lambda\to\infty$). The main differences between the two curves are that when $\lambda\to\infty$ the equilibrium value of θ is smaller. Plots for intermediate values of λ appear to have steps. These may be explained by gradual filling of the smaller gaps by binding with increasingly large overlaps. The clearest example is for the case λ$=100$ in Fig. 17 where five steps are clearly visible. The first step corresponds to nonoverlapped binding equilibrium (at $t=0.1$ s), the second when gaps of length $x-1=4$ sites are filled. Since the binding rate decreases by a factor of λ as the gap size decreases by one site, the second plateau occurs when $t=1$ s, the third when $t=100$ s, and so on.

The only difference between the parameters used to construct Figs. 17 and 18 is polymer length ($x=5$ in Fig. 17 and $x=10$ in Fig. 18). We note that convergence to equilibrium is slower when x increases (this is particularly evident when λ$=2$).

B. Irreversible binding capacity

When the binding rate varies with the gap size p according to (41), the binding capacity, that is the total number of polymers of length x which can be expected to adhere to a plasmid of length P_0, is

$$R(x,P_0)=1+\frac{2\sum_{p=1}^{P_0-x}R(x,p)+2\sum_{p=P_0-x+1}^{P_0-1}\lambda^{P_0-x-p}R(x,p)}{P_0-x+1+2\sum_{i=1}^{x-1}\lambda^{-i}} \quad (x\leqslant P_0), \tag{52a}$$

$$R(x,P_0)=1+\frac{2\sum_{p=1}^{P_0-1}\lambda^{P_0-x-p}R(x,p)}{(x-P_0-1)\lambda^{P_0-x}+2\sum_{i=x-P_0}^{x-1}\lambda^{-i}} \quad (2\leqslant P_0<x), \tag{52b}$$

$$R(x,1)=1. \tag{52c}$$

We recall that nonoverlapped binding is equivalent to size-dependent overlapped binding with λ$=\infty$ and note that Eq. (52a) reduces to Eq. (9a) in this case. Similarly Eq. (52a) reduces to Eq. (28) when λ$=1$. Equations (52) may be derived by considering all possible landing configurations of the polymers on the DNA plasmid. Figure 19 illustrates what cases may arise when the polymer is shorter than the DNA. The factor by which $k_f^{(x)}$ should be multiplied to determine the effective binding rate is given on the rhs.

There are P_0+x-1 landing positions (as in the case of constant-rate binding with overlaps), but these configurations occur with different probabilities because polymers are less

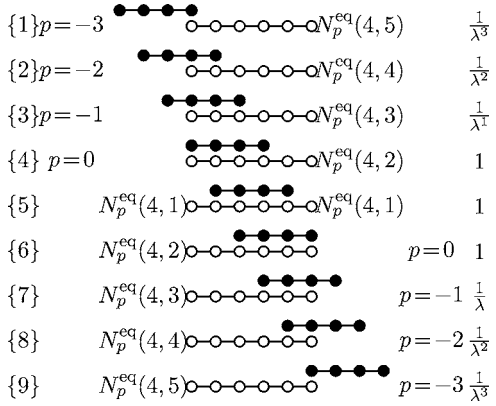

FIG. 19. Gap-length cooperativity of overlapped landing ($x=4$, $P_0=6$).

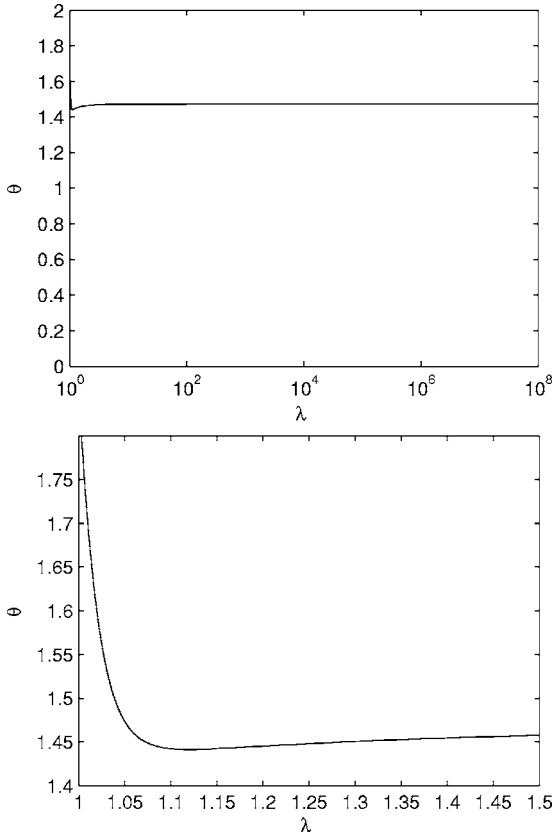

FIG. 20. Charge neutralization for the case of overlapped binding. Parameter values: $P_0=10\,000$, $x=100$.

likely to bind when they cannot adhere with all of their charges.

Figure 20 shows how the charge neutralization varies with λ when $P_0=10\,000$ and $x=100$. In the limit $\lambda\to\infty$ θ hardly changes from its value of 1.46 (which it attains at $\lambda=1.5$).

Note that there is no connection between the result derived in Sec. II D where $\theta<1$ and $\lambda=\infty$ and the asymptotic limit $\lambda\to\infty$ which gives $\theta\approx1.5$. Even for very large values of λ gaps of size $p<x$ are filled over very long time scales, the plasmid will eventually be completely covered in the limit $t\to\infty$ and have $\theta\geqslant1$. However, if $\lambda=\infty$, gaps of size $p<x$ are never filled and so $\theta\leqslant1\,\forall\,t$.

Figure 21 shows the equilibrium charge neutralization θ as a function of the polymer length x and cooperativity constant λ. As expected, increasing λ and/or x leads to an increase in θ.

C. Equilibrium gap distribution for variable-rate overlapped binding

Recursive relations for the equilibrium gap distribution $[N_p^{\mathrm{eq}}(x,P_0)]$ when there is variable-rate binding with overlaps are derived in this section. Figure 19 illustrates the derivation of the steady-state gap distribution when polymers of length $x=4$ land on a stretch of DNA of length $P_0=6$.

Let $N_{-3}^{\mathrm{eq}}(4,6)$ be the number of gaps of length −3 when polymers of length 4 land on a stretch of DNA which is six sites long. The relative rate at which each possible landing

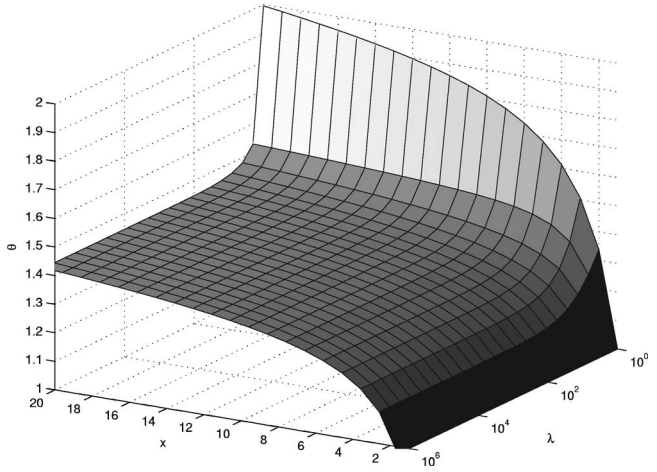

FIG. 21. Surface plot showing how, for a fixed value of P_0 ($P_0=2000$), the equilibrium charge neutralization θ changes as the polymer length x and binding cooperativity λ vary.

event occurs is shown on the right-hand side of Fig. 19. In this case the sum of the weights of all outcomes is

$$\omega=(1/\lambda^3+1/\lambda^2+1/\lambda+3+1/\lambda+1/\lambda^2+1/\lambda^3),$$

which generalizes to $(P_0-x+1+2\Sigma_{i=1}^{x-1}\lambda^{-i})$ for polymers of length x landing on gaps of length P_0.

The probability of a polymer landing in configuration {1} (see Fig. 19) is the rate at which this happens $(1/\lambda^3)$ normalized by the sum of all possible weights (ω), giving

$$\begin{pmatrix}\text{probability of}\\ \text{polymer landing in}\\ \text{configuration }\{1\}\end{pmatrix}=\frac{1/\lambda^3}{\omega}=\frac{1/\lambda^3}{1/\lambda^3+1/\lambda^2+1/\lambda+3+1/\lambda+1/\lambda^2+1/\lambda^3}.$$

This landing position creates one gap of length −3 but there is also the possibility of gaps of this size being created when polymers land on the remaining five-site gap. Therefore the total contribution to overlaps of length 3 from configuration {1} is

$$\frac{1/\lambda^3[1+N_{-3}^{\mathrm{eq}}(4,5)]}{\frac{1}{\lambda^3}+\frac{1}{\lambda^2}+\frac{1}{\lambda}+3+\frac{1}{\lambda}+\frac{1}{\lambda^2}+\frac{1}{\lambda^3}}.$$

Similar formulas hold for configurations {2}, {3}, {4}. Configuration {5} is a special case since two gaps are created. Hence the total contribution from {5} is

$$\frac{2N_{-3}^{\mathrm{eq}}(4,1)}{\frac{1}{\lambda^3}+\frac{1}{\lambda^2}+\frac{1}{\lambda}+3+\frac{1}{\lambda}+\frac{1}{\lambda^2}+\frac{1}{\lambda^3}}.$$

Arrangements {6}, {7}, {8}, {9} are identical to {4}, {3}, {2}, {1}. Combining the above results we deduce that

$$N_{-3}^{\mathrm{eq}}(4,6) = \frac{2}{\frac{1}{\lambda^3}+\frac{1}{\lambda^2}+\frac{1}{\lambda}+3+\frac{1}{\lambda}+\frac{1}{\lambda^2}+\frac{1}{\lambda^3}} \times \left(\frac{1}{\lambda^3}[1+N_{-3}^{\mathrm{eq}}(4,5)] + \frac{N_{-3}^{\mathrm{eq}}(4,4)}{\lambda^2} + \frac{N_{-3}^{\mathrm{eq}}(4,3)}{\lambda} + N_{-3}^{\mathrm{eq}}(4,2) + N_{-3}^{\mathrm{eq}}(4,1)\right). \tag{53}$$

Similar reasoning results in recursive relations for steady-state gap distributions for any polymer and DNA length. The number of gaps $N_p^{\mathrm{eq}}(x,P_0)$ of size p is determined by constructing a recurrence relation in which the length of the DNA molecule varies. We do this by first considering a DNA molecule of unit length ($\hat{P}_0=1$) and increasing $\hat{P}_0$ until $\hat{P}_0=P_0$. It is then possible to show that

$$N_p^{\mathrm{eq}}(x,P_0) = 2\frac{\lambda^p + \sum_{\hat{P}_0=1}^{P_0-x} N_p^{\mathrm{eq}}(x,\hat{P}_0) + \sum_{\hat{P}_0=P_0-x+1}^{P_0-1} \frac{N_p^{\mathrm{eq}}(x,\hat{P}_0)}{\lambda^{\hat{P}_0-P_0+x}}}{P_0-x+1+2\sum_{\hat{P}_0=1}^{x-1}\frac{1}{\lambda^{\hat{P}_0}}} \quad (x \leqslant P_0), \tag{54a}$$

$$N_p^{\mathrm{eq}}(x,P_0) = 2\frac{\lambda^p + \sum_{\hat{P}_0=1}^{P_0-1} \frac{N_p^{\mathrm{eq}}(x,\hat{P}_0)}{\lambda^{\hat{P}_0-P_0+x}}}{\frac{x-P_0+1}{\lambda^{x-P_0}} + 2\sum_{\hat{P}_0=1}^{P_0-1}\frac{1}{\lambda^{\hat{P}_0-P_0+x}}} \quad (p+x \leqslant P_0 < x), \tag{54b}$$

$$N_p^{\mathrm{eq}}(x,P_0) = 2\frac{\lambda^{P_0-x} + \sum_{\hat{P}_0=1}^{P_0-1} \frac{N_p^{\mathrm{eq}}(x,\hat{P}_0)}{\lambda^{\hat{P}_0-P_0+x}}}{\frac{x-P_0+1}{\lambda^{x-P_0}} + 2\sum_{\hat{P}_0=1}^{P_0-1}\frac{1}{\lambda^{\hat{P}_0-P_0+x}}} \quad (2 \leqslant P_0 < p+x), \tag{54c}$$

$$N_p^{\mathrm{eq}}(x,1) = \frac{2}{x}. \tag{54d}$$

Equations (54) allow us to investigate how gap distributions vary with λ. Plots of the gap distribution $N_p^{\mathrm{eq}}(x,P_0)$ for DNA of length $P_0=2000$, and polymer of length $x=50$ are shown in Fig. 22 for different values of λ. We note that when $\lambda=1$ a uniform distribution of gap lengths is observed; higher values of λ result in a greater proportion of smaller gaps, and increasing λ above 2 has little additional effect on the gap distribution.

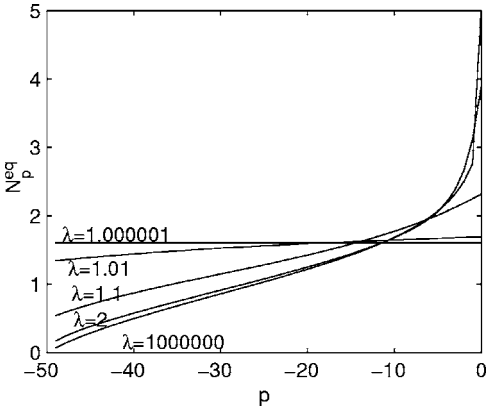

FIG. 22. Series of curves showing how the equilibrium gap distribution changes as the binding cooperativity λ varies. Parameter values: $P_0=2000$, $x=50$.

V. CONCLUSIONS

We have adapted an existing model of binding without overlaps [45] to construct new models of overlapped binding with constant and variable binding rates. We have shown that the simpler mechanism of overlapped binding gives rise to higher coverage in RSA than that allowed by standard RSA models. We believe that in systems such as polymer adsorption onto DNA, overlapped binding is a more likely mechanism than cooperative sequential adsorption (CSA), which is the other mechanism for acheiving the high charge neutralizations required for DNA condensation. In particular we point to charge inversion as the clinching argument, which is easily explained by overlapped binding but impossible both with standard RSA and even with CSA. Overlapped binding has some similarity with multilayer binding models analyzed by, for example, Bartelt and Privman [34] and Nielaba [35]. Ideally, of course, a mean field model encompassing both overlapped binding and multilayer adsorption would be useful.

Neither overlapped nor nonoverlapped irreversible binding scenarios lead to an "equilibrium" configuration, rather the dynamics simply leads to a final jammed state, which is degenerate. However, we have characterized the most likely final state using a mean-field approach. The method used in [28] to derive recurrence relations for the equilibrium charge neutralization has been generalized to determine equilibrium gap length distributions for nonoverlapped binding. Similar methods were used to study overlapped binding and to determine the associated charge neutralization and equilibrium gap length distribution. New exact expressions for DNA charge neutralization were derived for binding with overlaps and new asymptotic approximations for the case without overlaps were also obtained.

The numerical simulations of irreversible binding without overlaps presented here agree with previous work [26,27] in that they yield charge neutralizations that are insufficient to condense DNA. Our asymptotic formula for charge neutralization indicates that it is impossible to achieve the 90% charge neutralization required to condense the DNA [50] for any polymers when binding is irreversible and there are no

overlaps. It is possible to achieve 100% coverage with monomers but the counterion condensation model and experimental studies [23] suggest that such a combination would not condense. This is due to the fact that monomers being polymers of unit length would behave in a similar manner to monovalent ions, which are known not to cause DNA condensation. One hundred percent coverage with monomers is unlikely to be observed in realistic nonoverlapping systems due to monomers having nonzero unbinding and motion rates (giving rise to higher transational entropy).

Since DNA condensation by polymers is observed, there is something lacking in the traditional excluded site binding model: we believe that this is the phenomenon of overlapped binding. We have developed a model that describes the dynamics of the gap distributions that occur when polymers overlap and have shown that this allows higher charge neutralizations to occur than a model which forbids overlapped binding.

Furthermore, overlapped binding can explain charge inversion, where adhered polymers more than neutralize the DNA's negative phosphate charges, and form a complex with net positive charge. This phenomenon, where the charge neutralization ratio exceeds unity, which has been experimentally observed [42] and cannot be explained by nonoverlapped binding, is entirely consistent with our overlapped binding models.

Simulations involving irreversible binding with overlaps and a binding rate that is independent of the number of bound sites lead to much higher coverage of the DNA molecule than the nonoverlapping binding case.

In Sec. III C we constructed recurrence relations for the distribution of gaps and the charge neutralization for the case of irreversible binding with overlaps. We found that at equilibrium the gap sizes for overlapped binding were uniformly distributed. The binding rate was then modified to account for the number of sites to which the polymer binds. As a result, the steady-state charge neutralization reduced to more plausible levels.

In future work, the model of overlapped binding should be calibrated further by comparing experimental results with the solutions from our models to estimate the cooperativity parameter λ. Alternatively the model could be generalized further by imposing a limit on the smallest gap size in which a polymer can land. A more refined model would determine the rate's dependence on electrostatic DNA-polymer interactions and so be consistent with electrostatic/thermodynamic models of [51]. In forthcoming papers we explain how to generalize the theory and results outlined in this paper to the case of reversible polymer-binding and polymer motion along the DNA plasmid [36] and generalize all these results to the case of polymer mixtures in which the polymer lengths are nonuniform [37].

ACKNOWLEDGMENTS

We thank Snjezana Stolnik-Trenkic and Clive Roberts for helpful discussions and the BBSRC for financial support (EM).

[1] G. Brooks, *Gene Therapy. The Use of DNA as a Drug* (Pharmaceutical, London, UK, 2001).
[2] S. H. Cheng and R. K. Scheule, Adv. Drug Delivery Rev. **30**, 173 (1998).
[3] S. Ferrari, D. M. Geddes, and E. W. F. W. Alton, Adv. Drug Delivery Rev. **54**, 1373 (2002).
[4] R. C. Hoeben, Gene Therapy Mole. Biolo. **1**, 293 (1998).
[5] A. U. Bielinska, C. Chen, J. Johnson, and J. R. Baker, Jr., Bioconjugate Chem. **10**, 843 (1999).
[6] J. Widom and R. L. Baldwin, J. Mol. Biol. **144**, 431 (1980).
[7] S. T. Crooke, J. Drug Target. **3**, 185 (1995).
[8] I. MacLachlan, P. Cullis, and R. W. Graham, Curr. Opin. Mole. Therapeutics **1**, 252 (1999).
[9] R. Bruinsma and J. Mashl, Europhys. Lett. **41**, 165 (1998).
[10] C. Pouton, P. Lucas, B. Thomas, A. Uduehi, D. Milroy, and S. Moss, J. Controlled Release **53**, 289 (1998).
[11] V. A. Kabanov, V. G. Sergeyev, O. A. Pyshkina, A. A. Zinchenko, A. B. Zezin, J. G. H. Joosten, J. Brackman, and K. Yoshikawa, Macromolecules **33**, 9587 (2000).
[12] M. Ogris, P. Steinlein, S. Carotta, S. Brunner, and E. Wagner, AAPS PharmSci. **3**(3), E21 (2001).
[13] D. Porschke, Biochemistry **23**, 4821 (1984).
[14] E. Raspaud, I. Chaperon, A. Leforestier, and F. Livolant, Biophys. J. **77**, 1547 (1999).
[15] B. Bonnier, D. Boyer, and P. Viot, J. Phys. A **27**, 3671 (1994).
[16] A. Rényi, Publ. Math. Inst. Hung. Acad. Sci. **3**, 109 (1958).
[17] I. Gőssl, L. Shu, A. D. Schlűter, and J. P. Rabe, J. Am. Chem. Soc. **124**, 6850 (2002).
[18] U. Rungsardthong, "Physiochemical evaluation of polymer-DNA complexes for DNA. delivery," Ph.D. thesis, University of Nottingham, 2002.
[19] A. L. Martin, M. C. Davies, B. J. Rackstraw, C. J. Roberts, S. Stolnik, S. J. B. Tendler, and P. M. Williams, FEBS Lett. **480**, 106 (2000).
[20] B. J. Rackstraw, A. L. Martin, S. Stolnik, C. J. Roberts, M. C. Garnett, M. C. Davies, and S. J. B. Tendler, Langmuir **17**, 3185 (2001).
[21] H. Deng, V. A. Bloomfield, J. M. Benevides, and G. J. Thomas, Jr., Nucleic Acids Res. **28**, 3379 (2000).
[22] R. W. Wilson and V. A. Bloomfield, Biochemistry **18**, 2192 (1979).
[23] G. S. Manning, Q. Rev. Biophys. **2**, 179 (1979).
[24] I. Rouzina and V. A. Bloomfield, J. Phys. Chem. **100**, 4305 (1996).
[25] J. D. McGhee and P. H. von Hippel, J. Mol. Biol. **86**, 469 (1974).
[26] I. R. Epstein Biopolymers **18**, 765 (1979).
[27] I. R. Epstein, Biopolymers **18**, 2037 (1979).
[28] I. R. Epstein, Biophys. Chem. **8**, 327 (1978).
[29] P. D. Munro, C. M. Jackson, and D. J. Winzor, Biophys. Chem. **71**, 185 (1998).
[30] I. Rouzina and V. A. Bloomfield, Biophys. Chem. **64**, 139

(1997).
[31] S. H. Bossmann and L. S. Schulman, "Luminescence quenching as a probe of particle distribution," in *Nonequilibrium Statistical Mechanics in One Dimension*, edited by V. Privman (Cambridge U. P., Cambridge, 1997).
[32] J. W. Evans, "Random and cooperative sequential adsorption: exactly solvable problems on 1D lattices, continuum limits, and 2D extensions," in *Nonequilibrium Statistical Mechanics in One Dimension*, edited by V. Privman (Cambridge U. P., Cambridge, 1997).
[33] M. Barma, "Deposition-evaporation dynamics: jamming, conservation laws and dynamical diversity," in *Nonequilibrium Statistical Mechanics in One Dimension*, edited by V. Privman (Cambridge U. P., Cambridge, 1997).
[34] M. C. Bartelt and V. Privman, Int. J. Mod. Phys. B **5**, 2883 (1991).
[35] P. Nielaba, "Lattice models of irreversible adsorption and diffusion," in *Nonequilibrium Statistical Mechanics in One Dimension*, edited by V. Privman (Cambridge U. P., Cambridge, 1997).
[36] E. Maltsev, J. A. D. Wattis, and H. M. Byrne (unpublished).
[37] E. Maltsev, J. A. D. Wattis, and H. M. Byrne (unpublished).
[38] E. Ben-Naim and P. L. Krapivsky, J. Phys. A **27**, 3575 (1994).
[39] P. L. Krapivsky and E. Ben-Naim, J. Chem. Phys. **100**, 6778 (1994).
[40] C. P. Woodbury, Jr., Biopolymers **20**, 2225 (1981).
[41] J. Ray and G. S. Manning, Biopolymers **32**, 541 (1992).
[42] A. Y. Grosberg, T. T. Nguyen, and B. I. Shklovskii, Rev. Mod. Phys. **74**, 329 (2002).
[43] Y. Levin, Rep. Prog. Phys. **65**, 1577 (2002).
[44] S. Martins and J. F. Stilck, Physica A **311**, 23 (2002).
[45] E. R. Cohen and H. Reiss, J. Chem. Phys. **38**, 680 (1962).
[46] W. H. Press, S. A. Teukolsky, W. T. Vetterling, and B. P. Flannery, *Numerical Recipes in Fortran 90. The Art of Parallel Scientific Computing* (Cambridge U. P., Cambridge, 1996), Vol. 2.
[47] E. Maltsev, "Mathematical Modeling of DNA Condensation," Ph.D. thesis, University of Nottingham, 2005.
[48] J. J. González, P. C. Hemmer, and J. S. Hoye, Chem. Phys. **3**, 228 (1974).
[49] C.-H. Ahn, S. Y. Chae, Y. H. Bae, and S. W. Kim, J. Controlled Release **80**, 273 (2002).
[50] V. A. Bloomfield, Biopolymers **44**, 269 (1998).
[51] I. Rouzina and V. A. Bloomfield, J. Phys. Chem. **100**, 4292 (1996).